

Finding Achievable Region for Line Segment Obstacles

Aiden Zhijie Wang

Department of Computer Science and Engineering,
Shanghai Jiao Tong University, Shanghai, China
aiden.zjwang@gmail.com

Abstract. The problem of Finding Achievable Region (FAR) is a meaningful and novel problem, which is overlooked by previous researchers. Informally, given there are a set of obstacles in 2D space and a maximum path length (MPL), one (e.g., a person) walks freely from a starting point and stop to continue walk once the total travelled-distance is equal to MPL, we call the location (s)he stops as terminate point, the FAR problem is to find the union of all possible terminate points. In this paper, we first propose and formulate this problem, followed by presenting a slice based method for tackling this problem. We prove the correctness of our proposed method, and demonstrate that the method takes $O(N^3 \log N)$ time for the FAR problem.

1 Introduction

The problem of *Finding Achievable Region*(FAR), viewing from different perspective, is similar to the following several classical problems, *Visibility Polygon* problem [1], *Visibility Graph* problem [2], *Art Gallery* problem [3], *Watchman Route* problem [4], *Sensor Coverage* problem [5,6] and the *Motion Planning* problem [7], etc. For these classical problems, which have been well studied and a large bulk of solutions can be found in recent publications [8,5]. The FAR problem is a novel problem, which is overlooked by previous researchers. For ease of discussion, we, in here, present a visual example to illustrate what the FAR problem is.

The black point is the starting point, the maximum path length (MPL) is the radius of the circle, and we assume the black line segment is an obstacle as shown in Figure 1(a). Figure 1(b) illustrates the result of FAR, i.e., all the locations in the circle are achievable except the locations in the white region. Therefore, the achievable region (AR) is the subtraction between the circle and the white region. Note that, in this example, there is only one obstacle, in this case we can obtain the result easily. However, once there are a large number of obstacles like Figure 1(c) illustrates or more complicate cases, the FAR problem will turn into rather complicate. In this paper, our goal is to develop an accurate and efficient method for tackling the FAR problem.

The FAR problem can be took as a promising problem since it can be mapped to many application scenarios. For instance, assuming that a criminal gangs robbed a bank at 3 a.m. and now they are running away by riding “Toyota

Royal V6”, then, based on the geographical information around the bank, the maximum speed of the criminal car and the elapsed time, the policeman can get the *achievable region* the criminals may locate, which will contribute to the reduction of search range, note that, a more tight search scope will save more search cost in terms of manpower and time; or assuming that there is a lost child, someone told his mother that (s)he have seen the child in position “A” an hour ago, then, based on geographic information around location “A” and the maximum speed that the child can walk, the mother can get the *achievable region* her child may locate, then she may turn to her relatives for help and seek the lost child in the *achievable region*. In our real life, there are many application scenarios like the above two examples, we do not further enumerate them for saving space. People possible argue that the criminal car or the lost child is continuous moving, and the obstacles possible are various geometries in addition to line segments. Certainly, it is needed to consider these factors in real applications. It is worth noting, the examples we presented above just illustrate the potential application scenarios for the FAR problem. In addition, line segment is the most elemental element for various geometries. In this paper, we are interesting in line segment obstacles.

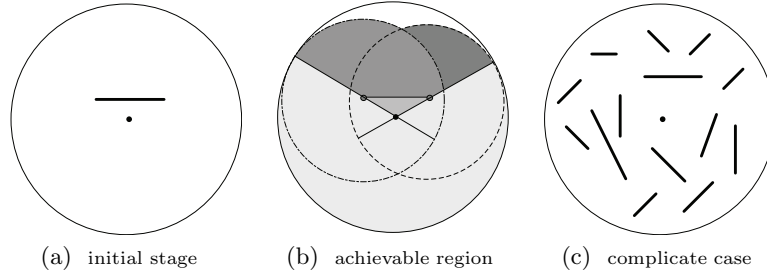


Fig. 1. Example of Finding Achievable Region

For tackling the FAR problem, there are two main challenges. Data representation for *achievable region* as well as intermediate result is a vital issue that we should make well consideration. Taking Figure 1(b) for example, the *achievable region* is the subtraction between the big circle and the white region, then, how to represent the result of this subtraction, or how to represent the white region? Another main challenge is the design of algorithm, that is, how to develop an algorithm that can efficiently and accurately find out the achievable region?

Motivate by the above presentation, we, in this paper, investigate the FAR problem. To sum up, we make the following contributions.

- We first propose and formulate the FAR problem.
- We delve into the details of this problem, and develop an efficient and accurate approach for tackling it.
- We, through theoretical analysis, prove the correctness of our proposed method and demonstrate its’ computational complexity.

The rest of the paper is organized as follows. In Section 2, we review related works. We, in Section 3, formally formulate this problem and introduce the main notations used in this paper. In section 4, we present a slice based method for solving the FAR problem. In particular, we prove the correctness of our proposed method and analyse its computational complexity. Finally, we conclude this paper and present our future research directions in Section 6.

2 Related Works

There are several classical problems (such as visibility polygon problem and Sensor coverage problem) which are most related to the FAR problem. To some extent, these problems can be classified into two categories: computation of visibility and coverage problem.

2.1 Computation of Visibility

Visibility is a mathematical abstraction of the real-life notion of visibility. Given a set of obstacles in the Euclidean space, two points in the space are said to be visible to each other, if the line segment that joins the two points does not intersect any obstacles. Computation of visibility is among the basic problems in computational geometry and has many applications in computer graphics, motion planning, and other areas [8]. Specifically, there are several classical problems which can be view as the variants of visibility problem.

One of variant is the visibility polygon problem, in particular, the visibility polygon or visibility region for a point, say p , in the plane among non-transparent obstacles possible is an unbounded polygonal region, which is consisted of all points of the plane visible from p . On the other hand, if the visibility polygon is bounded then it is a star-shaped polygon [1]. The visibility graph problem is another variant, a visibility graph is a graph of inter-visible locations, typically for a set of points and obstacles in the Euclidean plane. Each node in the graph represents a point location, and each edge represents a visible connection between them [2]. Moreover, the art gallery problem or museum problem also is a well-studied visibility problem, which originates from a real-world problem of guarding an art gallery with the minimum number of guards which together can observe the whole gallery [3]. The watchman route problem is an optimization problem where the objective is to compute the shortest route a watchman should take to guard an entire area with obstacles given only a map of the area. The challenge is to make sure the watchman peeks behind every corner and to determine the best order in which corners should be visited in. There are polynomial-time solutions but they all suffer from severe numerical problems inherent in the computations [4]. Last but not least, the motion planning problem is to produce a continuous motion that connects a start configuration \mathbb{S} and a goal configuration \mathbb{G} , while avoiding collision with known obstacles. The robot and obstacle geometry is described in a 2D or 3D workspace, while the motion is represented as a path in configuration space [7].

Beside the above problems can be classified into the computation of visibility, fortress problem [9], hidden line removal problem [10] and hidden surface removal problem [11] can also be classified into this category. Obviously, all these problem are different from the FAR problem.

2.2 Coverage Problem

The term “coverage” is used in many fields. For instance, *fault coverage* in VLSI [12], *fold coverage* in genetic sequencing [13], *code coverage* in software testing [14], etc. In here, we mainly refer to the coverage problem in sensor networks.

Coverage which is one of the most important performance metrics for sensor networks reflects how well a sensor field is monitored. Individual sensor coverage models are dependent on the sensing functions of different types of sensors, while network-wide sensing coverage is a collective performance measure for geographically distributed sensor nodes [5,6]. Though coverage problem in sensor network and the FAR problem share some similarities since both of the problems involve the concept of “region”, it is not difficult to find that they are different in essence.

3 Problem Definition and Notations

At first we give the definition of *path length* before we formally define the problem of *finding achievable region*.

Definition 1. *Given a starting point, SP , and a terminate point, TP , in 2D space, one freely walks from SP to TP , the **path length** is the total travelled-distance from SP to TP .*

Note that, if the SP and TP is the same point in 2D space, the *path length* is not definitely equal to 0. For example, given two different locations, say A and B , in 2D space, and we assume that both SP and TP are in location A , if one person firstly walks from A to B , and walks back from B to A , then, the *length path* is larger or equal to $2 * \|\text{dis}(A, B)\|$, where $\|\text{dis}(A, B)\|$ denotes the Euclidean distance between the two locations A and B .

Definition 2. *Given there are a set N of obstacles in 2D space. For any two obstacles O_i and O_j ($i \neq j$, $1 \leq i, j \leq N$), we assume $O_i \parallel O_j$ (i.e., the intersection of the two obstacles is \emptyset). Given a starting point, SP ($SP \notin \bigcup_{i=1}^N O_i$), the maximum value of path length is MPL . One starts (from the SP) to freely walk but cannot directly pass through any obstacle, and stop to continue walk once the travelled-distance is equal to MPL . The problem of **Finding Achievable Region** is to find all the possible locations (or points) it can reach at when SP and MPL is given beforehand.*

Note that, the obstacles, in real-world, possible are various geometries such as rectangle, circle, ellipse, trapezoid, line segment, even to other irregular shapes.

Table 1. Main symbols used in this paper

symbols	Description
N	number of obstacles
O_i	the i obstacle
CAR	candidate achievable region
COs	candidate obstacles
AR	achievable region
MPL	maximum path length
S_j	the j slice
AAR_j	accurate achievable region in S_j

Since line segment is the most elemental element for other geometries, we, in this paper, only consider the obstacles are line segments, it will lay a foundation for further investigating the generic case, that is, the obstacles are arbitrary shapes. In the rest of this paper, if without stating otherwise, we use obstacle(s) to substitute line segment obstacle(s), and we assume we have indexed all obstacles in a data structure, such as R-tree, based on their MBRs. For convenience, we summarize the main symbols in Table 1.

4 Slice Based Method

For tackling the FAR problem, a slice based method is proposed, we first introduce the framework followed by presenting the details.

4.1 Framework

The framework of our solution is illustrated in Figure 2. Specifically, we first let the circle centering at SP and with radius MPL as candidate achievable region (CAR), and use the CAR to prune those unrelated obstacles and unrelated part of some obstacles, thus obtain the candidate obstacles (COs) (line 1-2). Next, we divide the CAR into multiple parts based on slicing rules (line 3). Then, we evaluate accurate achievable region (AAR) for each slice S_j , after we dealt with each slice, we combine all the AARs from each slice and return the result at last (line 4-7).

4.2 Pruning Unrelated Obstacles

It is easy to know that AR is equal to CAR when there is no any obstacle, and AR must be a subset of CAR (i.e., $AR \subseteq CAR$) once there exist obstacle(s). For instance, in Figure 1(b), the non-white region (corresponding to AR) is a subset of the big circle (corresponding to CAR). Therefore, at the beginning of evaluating the AR, we can use the CAR to prune some unrelated obstacles. Specifically, there are three types of obstacles that should be pruned or be pruned partially.

```

Procedure Framework_FAR {
  Input:  $\sum_{i=1}^N O_i, MPL, SP$ 
  Output:  $AR$ 
  (1)  $AR \leftarrow \emptyset, CAR \leftarrow$  circle centering at  $SP$  and with radius  $MPL$ 
  (2) prune unrelated obstacles and part of obstacles
  (3) divide  $CAR$ , based on slicing rules, into  $k$  slices,  $S_1, S_2, \dots, S_k$ 
  (4) For  $j = 1$  to  $k$ 
  (5)    $AAR_j \leftarrow$  evaluate the accurate achievable region in  $S_j$ 
  (6)  $AR \leftarrow \bigcup_{j=1}^k AAR_j$ 
  (7) return  $AR$  }

```

Fig. 2. Framework of Finding Achievable Region

Lemma 1. *Given there are a number N of obstacles in 2D plane, let circle centering at SP with radius MPL be the CAR . Any obstacle O_i ($1 \leq i \leq N$) can be safely pruned if $O_i \uparrow\uparrow CAR$ (i.e., O_i and CAR are disjoint).*

Proof. We only need to prove any sub-segment of the obstacle O_i makes no impact on the AR under the assumption that $O_i \uparrow\uparrow CAR$. Without loss of generality, we cut O_i into m segments, say s_1, s_2, \dots, s_m , and we assume s_k ($1 \leq k \leq m$) is the nearest sub-segment to CAR . Since $s_k \in O_i$ and $O_i \uparrow\uparrow CAR$, we have $s_k \uparrow\uparrow CAR$, i.e., any point $p \in s_k$, it has $p \notin CAR$. Therefore, $dist(p, SP) > MPL$ ¹, which means that one definitely cannot reach at the point p . Since $p \in s_k$, and we assume p is an any point, we can conclude that one definitely cannot reach at s_k . Further, since we assume s_k is the nearest sub-segment to CAR , based on analysis geometry, we have that one definitely cannot reach at any other sub-segment s_r ($r \neq k$ and $1 \leq r \leq m$), either. In summary, any sub-segment of O_i makes no impact on the AR. \square

For example, line segments (h, i) and (o, p) in Figure 3(a) should be pruned since $(h, i) \uparrow\uparrow CAR$ and $(o, p) \uparrow\uparrow CAR$, too.

Lemma 2. *Given there are a number N of obstacles in 2D plane, let circle centering at SP with radius MPL be the CAR . If an obstacle O_i intersects with the CAR , and assume O_i is subdivided into a number of sub-segments by the crossing point(s), then, all sub-segment(s) that is/are not inside the CAR can be safely pruned.*

Proof. We only need to prove any sub-segment, say s_k ($\notin CAR$), makes no impact on AR, the proof can be derived based on lemma 1. \square

Taking line segment (a, c) in Figure 3(a) as an example, since (a, c) intersects with CAR at point b and $(a, b) \notin CAR$, so line segment (a, c) should be pruned partially, namely, sub-segment (a, b) will be removed.

Lemma 3. *Given there are a number N of obstacles in 2D plane, let circle centering at SP with radius MPL be the CAR , and given an obstacle O_j divides the CAR into two parts, Part1 and Part2, and assume $SP \in Part1$. Any obstacle O_i ($1 \leq i \leq N$ and $i \neq j$) can be safely pruned if it lies in the side of Part2.*

¹ $dist(p, SP)$ is the Euclidean distance between the two points p and SP .

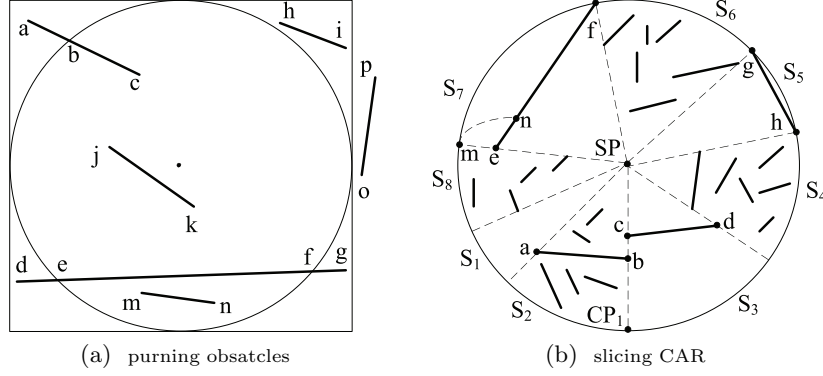


Fig. 3. Example of Pruning and Slicing

Proof. Due to the limitation of obstacle O_j , one cannot enter into the side of *Part2* if (s)he do not walk out of the CAR. Otherwise, if (s)he enters into the side of *Part2* by walking out of the CAR, the travelled-distance will be larger than MPL, which is contrary to the given condition. Therefore, any obstacle that is locating in the side of *Part2* makes no impact on the AR. \square

As an example, line segment (d, g) in Figure 3(a) subdivides the CAR into two parts, SP lies in the upper part, however, line segment (m, n) lies in the lower part, so (m, n) should be pruned. For the three types of obstacles discussed just now, we prune or partially prune according to the following method.

First, we, using the MBR of CAR as the input, search on the constructed index structure, which indexing the MBRs of all obstacles, in this way, we can obtain the initial candidate obstacles (ICOs). As an example, the square illustrates the MBR of CAR as shown in Figure 3(a), line segment (o, p) will be pruned since its' MBR and the MBR of CAR are disjointed, all the rest of obstacles in Figure 3(a) are ICOs. Next, we, according to their spans², sort all the ICOs in the descending order, and then deal with the sorted ICOs one by one. The reason we sort the ICOs is convenient for pruning correctly those obstacles that are relevant with the CAR but are irrelevant with the evaluation of AR. Taking line segment (m, n) in Figure 3(a) as an example, it lies in CAR, but it is irrelevant with the evaluation of AR. If we deal with (m, n) prior to (d, g) , the (m, n) possible cannot be pruned correctly. After we dealt with each ICOs, in the end, we obtain the candidate obstacles (COs). For example, the COs in Figure 3(a) will be (b, c) , (j, k) , and (e, f) .

The algorithm for pruning unrelated obstacles is illustrated in Figure 4. Note that, when we deal with the sorted ICOs one by one (line 3-11), we differentiate two cases. 1) All obstacles that have been processed cannot subdivide CAR into two parts (line 4-5). 2) There is at least one obstacle that has been processed and can subdivide CAR into two parts (line 6-11). The subprocedure

² if a line segment, say (a, b) , is parrallel to x-axis (or y-axis), the span is $dist(a, b)$. Otherwise, the span is $MAX(\|a.x - b.x\|, \|a.y - b.y\|)$, where $a.x$ is the horizontal ordinate of endpoint a .

```

Procedure Pruning_Obstacles {
  Input:  $\sum_{i=1}^N O_i$ , CAR
  Output: COs
  (1) ICOs  $\leftarrow$  use MBR of CAR to prune obstacle(s),  $switch \leftarrow 0$ , BSLs  $\leftarrow \emptyset$ 
  (2) sort all the ICOs based on their spans
  (3) for each obstacle  $O_i$  in ICOs
  (4)   if ( $switch = 0$ ) then //no obstacle ever divided CAR into 2 parts
  (5)     Subprocedure Handle_Obstacle ( $O_i$ , CAR, BSLs,  $switch$ )
  (6)   else //obstacle ever divided CAR into two parts
  (7)     for each BSL in BSLs // BSL can divide CAR into two parts
  (8)       if ( $O_i$  lies in unachievable part) then
  (9)         remove  $O_i$  from ICOs, break;
  (10)    if ( $O_i$  has not been removed) then
  (11)      Subprocedure Handle_Obstacle ( $O_i$ , CAR, BSLs,  $switch$ )
  (12) COs  $\leftarrow$  ICOs
  (13) return COs }

  Subprocedure Handle_Obstacle {
  Input:  $O_i$ , CAR, BSLs,  $switch$  // BSLs (Big Split Lines)
  (14) if ( $O_i$  and CAR are disjointed) then remove  $O_i$  from ICOs
  (15) else if ( $O_i$  lies in CAR) then // do nothing
  (16) else //  $O_i$  intersects with CAR
  (17)   if (there are two crossing point) then
  (18)     BSL  $\leftarrow O_i$ , BSLs  $\leftarrow$  BSLs  $\cup$  BSL
  (19)     if ( $switch = 0$ ) then  $switch = 1$ 
  (20)    $O_i \leftarrow$  cut off the unrelated part of  $O_i$  // i.e., the part that outside the CAR }

```

Fig. 4. Algorithm for Pruning Unrelated Obstacles

Handle_Obstacle() is straightforward, only one thing is needed to mention, that is, 'BSLs' is used for storing those obstacles that have been processed and can subdivide CAR into two parts.

4.3 Slicing and Placing

Up to now, we obtained the COs, in this subsection, we discuss slicing and placing. On the whole, we divide the CAR into multiple parts (or sectors) based on the *slicing lines* (SLs) defined later, and place the COs into corresponding parts.

Definition 3. *Given a candidate obstacle CO_i , its' endpoints are $CO_{i.1}$ and $CO_{i.2}$, respectively. We connect SP with $CO_{i.1}$ / $CO_{i.2}$, and extend line segment $(SP, CO_{i.1})$ / $(SP, CO_{i.2})$ along the direction of SP to $CO_{i.1}$ / $CO_{i.2}$ until it intersects with the border of CAR at a point, say $CP_{i.1}$ / $CP_{i.2}$. If line segment $(SP, CP_{i.1})$ / $(SP, CP_{i.2})$ does not pass through other obstacles except the endpoint(s) of obstacle(s), then the line segment $(SP, CP_{i.1})$ / $(SP, CP_{i.2})$ is a **Slicing Line**.*

Lemma 4. *Given a candidate obstacle CO_i , it can produce two SLs at most, and 0 SL at least.*

Proof. Since CO_i has only two endpoints, and based on Definition 3, the proof can be derived. \square

For example, the dashed lines in Figure 3(b) illustrate all the 8 SLs, line segment (a, b) produces two SLs, however, those small line segments produce 0

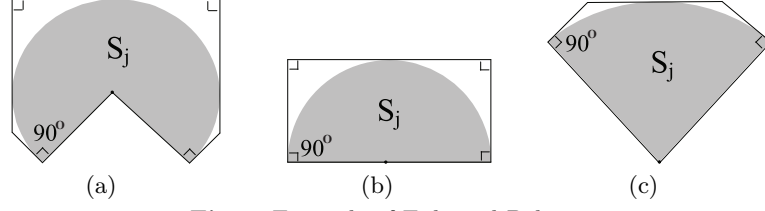


Fig. 5. Example of Enlarged Polygon

SL. For getting all the SLs, a straightforward solution is that, for each CO, we verify if it can produce SL(s), if so, we save the new produced SL(s), until we verified all the COs. Note that, though a SL cannot pass through other obstacles, but it can touch the endpoint(s) of other obstacle(s) as shown in Definition 3. So, we have

Lemma 5. *Given line segment $(SP, CP_{i.1})$ is a SL, which is the extended line segment of $(SP, CO_{i.1})$, where $CO_{i.1}$ is an endpoint of candidate obstacle CO_i , if $(SP, CP_{i.1})$ passes through an endpoint, $CO_{j.1}$, of another candidate obstacle CO_j , then the two candidate obstacles, CO_i and CO_j , share a common SL.*

Proof. We only need to prove the following two claims. (1) CO_j can produce a SL by endpoint $CO_{j.1}$. (2) The SL produced by the endpoint $CO_{j.1}$ is coinciding with $(SP, CP_{i.1})$.

Based on Definition 3, we construct an extended line segment, say $(SP, CP_{j.1})$, from $(SP, CO_{j.1})$. We first prove $(SP, CP_{j.1})$ is coinciding with $(SP, CP_{i.1})$. Since $(SP, CP_{j.1})$ is extended from line segment $(SP, CO_{j.1})$, obviously, $(SP, CP_{j.1})$ passes through the point $CO_{j.1}$. In addition, we know from the given condition that $(SP, CP_{i.1})$ pass through the endpoint $CO_{j.1}$. So, we have that the $(SP, CP_{i.1})$ and $(SP, CP_{j.1})$ pass through two common points, i.e., SP and $CO_{j.1}$. Moreover, both $(SP, CP_{i.1})$ and $(SP, CP_{j.1})$ are the radius of CAR, Therefore, $(SP, CP_{j.1})$ is coinciding with $(SP, CP_{i.1})$.

Next, we prove $(SP, CP_{j.1})$ is a SL by contradiction. Assume $(SP, CP_{j.1})$ is not a SL. However, we have proved that $(SP, CP_{j.1})$ is coinciding with $(SP, CP_{i.1})$, then $(SP, CP_{i.1})$ is not a SL. It is contrary to the given condition. Hence, the lemma holds. \square

Lemma 5 indicates that if a SL passes through an endpoint of other candidate obstacle, then this endpoint will be free from being verified. Taking candidate obstacle (a, b) in Figure 3(b) as an example, it produces a SL, i.e., (SP, CP_1) , since (SP, CP_1) passes through the endpoint c of candidate obstacle (c, d) , Therefore, for endpoint c , we need not verify it in the future. In addition, from Lemma 5, we have an immediate corollary below.

Corollary 1. *If a SL passes through a number K of endpoints of other candidate obstacles, then all the K endpoints will be free from being verified.* \square

```

Procedure Slicing.Placing {
  Input: CAR, COs, SP
  Output:  $\sum_{j=1}^{\|SLs\|} S_j.CO_s$  // all COs has been put into corresponding sectors.
  (1)  $SLs \leftarrow \emptyset, RLT \leftarrow \emptyset$  //  $RLT$  means repetitive label table
  (2) for each CO  $\in$  COs
  (3)   for each endpoint  $CO.k$  of CO //  $k = 1, 2$ 
  (4)     if ( $CO.k \notin RLT$ ) then
  (5)       if ( $CO.k$  can produce an new SL) then
  (6)          $SL_i \leftarrow$  the new produced SL,  $SLs \leftarrow SLs \cup SL_i$ 
  (7)         if ( $SL_i$  passes through other endpoint(s)) then
  (8)            $RLT \leftarrow RLT \cup$  (the(se) endpoint(s))
  (9)       else //  $CO.k \in RLT$ 
  (10)        remove  $CO.k$  from  $RLT$ 
  (11)  $\sum_{j=1}^{\|SLs\|} S_j \leftarrow$  divide CAR into a number  $\|SLs\|$  of sectors based on the SLs
  (12) for  $j = 1$  to  $\|SLs\|$ 
  (13)    $S_j.CO_s \leftarrow \emptyset$  //  $S_j.CO_s$  for storing COs that lie in sector  $S_j$ 
  (14)    $EP_j \leftarrow$  compute the enlarged polygon of  $S_j$ 
  (15)   for each CO  $\in$  COs
  (16)     for each  $EP_j \in \sum_{j=1}^{\|SLs\|} EP_j$ 
  (17)       if (CO lies in  $EP_j$ ) then  $S_j.CO_s \leftarrow S_j.CO_s \cup CO$ ; break ;
  (18) return  $\sum_{j=1}^{\|SLs\|} S_j.CO_s$  }

```

Fig. 6. Algorithm for Slicing and Placing

In the end, all the SLs are obtained, these SLs divide the CAR into multiple regions, i.e., sectors. For example, there are 8 sectors as shown in Figure 3(b). Once the CAR is divided into multiple sectors, next, we place all the COs into corresponding sectors, the method to place COs is as follows.

First, for each sector S_j , we compute its' enlarged polygon, EP_j , such that (1) $S_j \subset EP_j$, and (2) any $CO \in EP_j$, it can ensures $CO \in S_j$, where $1 \leq j \leq \|SLs\|$. Note that, an enlarged polygon with less edges will contribute to the follow-up calculations, we use an example, as shown in Figure 5, to illustrate how to obtain an enlarged polygon from a sector. Polygon in Figure 5(a) illustrates the enlarged polygon where S_j is a major-arc sector, similarly, polygons in Figure 5(b) and Figure 5(c) illustrate the enlarged polygons where the two sectors are a semi-circle sector and a minor-arc sector, respectively. The reasons we obtain EP_j is that to determine “ $CO \in EP_j$ ” is more simple than to determine “ $CO \in S_j$ ”.

Next, for each CO, we verify the CO is locating in which “ EP_j ”, it can be achieved by testing whether a EP_j contains both of the endpoints of the CO. If so, we place the CO in sector S_j , which is corresponding to the enlarged polygon EP_j . In this way, all COs will be placed in their corresponding sectors.

Figure 6 depicts the algorithm for slicing and placing. Specifically, “line 1-11” is used for slicing the CAR, “line 12-17” is used for placing the COs into their corresponding sectors. Note that, ‘ RLT ’ is used for storing the endpoints that are sharing a common SL, as Lemma 5 claims.

4.4 Evaluation of AAR

It is easy to know, given we can obtain the accurate achievable region (AAR) in each sector, the AR can be obtained by merging all the AARs. In this subsection, we discuss how to obtain the AAR.

Generally speaking, we can classify the sector S_j into four cases according to the candidate obstacle(s) it contains.

- **Case 1:** There is no CO locating in S_j . In this case, the AAR is equal to the sector S_j . For example, the AAR in S_1 is equal to S_1 as shown in Figure 3(b).
- **Case 2:** One CO lies in S_j , and both of the endpoints of the CO touch the border of CAR. In this case, the AAR is equal to a triangle. For example, the AAR in S_5 is equal to $\triangle(SP, g, h)$ as shown in Figure 3(b).
- **Case 3:** One CO lies in S_j , and only one endpoint of the CO touches the border of CAR. In this case, the AAR is equal to the union of two regions, which are a triangle and a small sector, respectively. For instance, the AAR in S_7 is the union of $\triangle(SP, e, f)$ and small sector $\angle(e, m, n)$, as shown in Figure 3(b).
- **Case 4:** All the the rest of situations, which including:
 - One CO lies in S_j , and no endpoint of the CO touches the border of CAR. E.g., S_3 in Figure 3(b).
 - There is no less than two COs locating in S_j . E.g., S_2, S_4, S_6 and S_8 in Figure 3(b).

Among the four cases, to evaluate the AAR for the first three cases is straightforward as presented above, however, for case 4, it is a complicate situation especially when there are a large number of COs in S_j . In the sequel, we address the method computing AAR for case 4. The algorithm for computing AAR is depicted in Figure 7. Simply to speaking, there are several steps. First, for each endpoint of each CO in S_j , we evaluate the shortest path (STP) from SP to the endpoint (line 2-4). Second, we find the visibility region, $VR_{i.k}$, of the endpoint in enlarged polygon EP_j if STP is less than the MPL (line 6). Third, we let the subtraction between MPL and STP be the rest of walking length (RWL), and use the circle centering at the endpoint with radium RWL to prune the visibility region, termed the pruned result as $PVR_{i.k}$ (line 7-10). Fourth, we combine all the pruned visibility regions (PVRs) and return the AAR in S_j (line 11-12).

```

Procedure Computing_AAR {
  Input:  $S_j.CO_s, S_j, EP_j, SP, MPL$ 
  Output: AAR
  (1) AAR  $\leftarrow \emptyset$  // constructing visibility graph in this step will be more efficient.
  (2) for  $i = 1$  to  $\|S_j.CO_s\|$ 
  (3)   for each endpoint  $CO_{i.k}$  of  $CO_i$  //  $k = 1, 2$ 
  (4)     STP  $\leftarrow$  the shortest path from  $SP$  to this endpoint
  (5)     if (STP < MPL) then
  (6)        $VR_{i.k} \leftarrow$  evaluate the visibility region from the endpoint,
  (7)       RWL  $\leftarrow MPL - STP$ 
  (8)        $TempC \leftarrow$  circle centering at  $CO_{i.k}$  with radium RWL
  (9)        $PVR_{i.k} \leftarrow VR_{i.k} \cap TempC$  // prune those unachievable region
  (10)      put  $PVR_{i.k}$  into  $PVRs$  //  $PVRs$  is used for storing
  (11) AAR  $\leftarrow$  computing the union of all PVRs stored in  $PVRs$ 
  (12) return AAR }

```

Fig. 7. Algorithm for Computing AAR

Lemma 6. *Given any sector S_j , which consists of a circular arc and two SLs, say SL_1 and SL_2 , and given we have obtained the AAR in S_j , say AAR_j , then, no matter how complicate the boundary of AAR_j is, it always include two edges, SL_1 and SL_2 .*

Proof. If the S_j is belonging to case 1, or 2, or 3 sector, it is obvious as shown in Figure 3(b). Even if the S_j is belonging to case 4 sector, any point on the two SLs is achievable based on Definition 3, so, any point on the two SLs must be included in AAR_j . In addition, since $AAR_j \subseteq S_j$ always hold, and SL_1 and SL_2 are the boundary of S_j . Then, SL_1 and SL_2 must be the boundary of AAR_j . Thus, the lemma holds. \square

From Lemma 6, we have an immediate corollary below.

Corollary 2. *Given any two adjacent sector S_j and S_j^* , they share a common SL, say SL_1 , the AARs in S_j and S_j^* are AAR_j and AAR_j^* , respectively. Then AAR_j and AAR_j^* also share a common edge, this edge just is the SL_1 . \square*

In above algorithm (cf. Figure 7), there are two sub-tasks, “calculating shortest path from SP to the endpoint $CO_{i.k}$ ” and “evaluating visibility region from the endpoint $CO_{i.k}$ in EP_j ”, which are the key of points. In order to better understand the two sub-problems, we explain the details in the sequel.

Visibility region of endpoint $CO_{i.k}$ in EP_j one classical and easy-to-implement method for computing visibility region is ray-sweeping. Though most existing algorithms for finding visibility region are focusing on the situation where the obstacles are polygons, their ideas can be easily incorporated into this sub-problem. First, we draw ray from endpoint $CO_{i.k}$ toward the endpoint, say $CO_{j.k}$, of other line segments that are locating in EP_j . For clearness, we call this ray as $R_{(CO_{i.k}, CO_{j.k})}$. There are three cases as follows.

- **Case 1:** The ray passes through nothing before it reaches at $CO_{j.k}$, but passes through other line segment(s) ³, before it reaches the border of EP_j . For ease of discussion, we call the first line segment the ray passes through as CO_f .
- **Case 2:** The ray passed through other line segment before it reaches at the endpoint $CO_{j.k}$.
- **Case 3:** The ray passed through nothing except $CO_{j.k}$ before it reaches the border of EP_j .

If the ray belongs to case 2, we discard it. For case 1, we compute the crossing point between the ray and CO_f , and store this crossing point. For case 3, we compute the crossing point between the ray and EP_j , and store this crossing point. Moreover, for all ‘case 1’ and ‘case 3’ rays, we sort them in the direction of counter-clockwise w.r.t. polar plane coordinate. Then, the visibility region can be constructed based on the border of EP_j and a series of crossing points and endpoints. We use an example to illustrate the procedure of constructing visibility region.

³ In here, if the ray only passes through the endpoint of other line segment, we consider it passes through nothing. That is, we do not take it as ‘case 1’ ray.

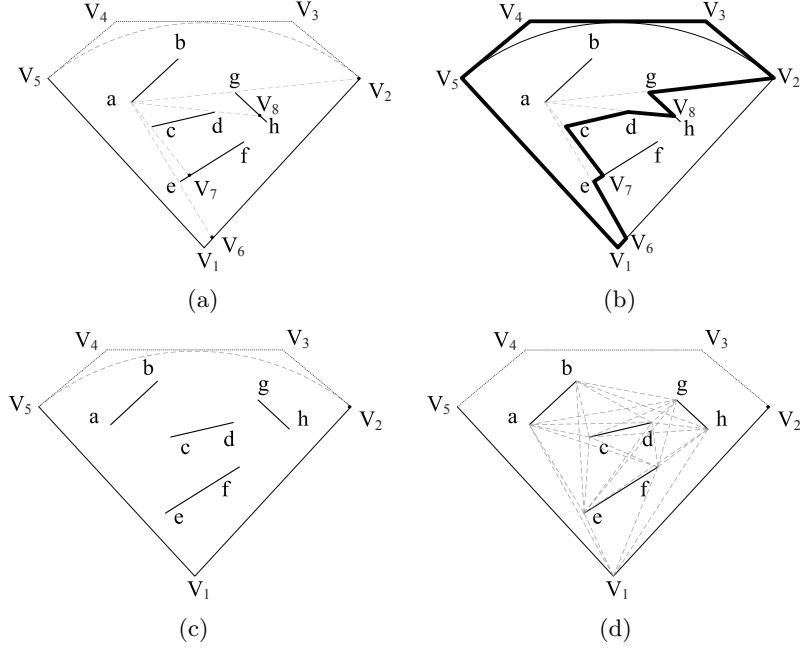


Fig. 8. Example of Visibility Region and Visibility Graph

For example, polygon $(V_1, V_2, V_3, V_4, V_5)$ illustrates the EP_j , and the endpoint a illustrates the $CO_{i,k}$ as shown in Figure 8(a). For obtaining the visibility region, at first, we draw ray from endpoint a toward the endpoints of other line segments that are locating in EP_j . In here, $R_{(a,e)}$ and $R_{(a,g)}$ belong to the 'case 3' ray, they intersect with EP_j at V_6 and V_2 , respectively. $R_{(a,c)}$ and $R_{(a,d)}$ belong to the 'case 1' ray, they intersect with line segment (e, f) at V_7 , and with line segment (g, h) at V_8 , respectively. Given we construct the visibility region starting from the $R_{(a,e)}$ and traversing according to the direction of counter-clockwise, then, V_6 first is inserted into the resultant list, next, e is inserted. For $R_{(a,c)}$, we insert V_7 followed by inserting c , since V_7 and e are on the same line segment (e, f) , as well as e has been inserted just now. Similarly, d, h, g and V_2 are inserted orderly. In this time, all rays are dealt with, we then insert the rest of vertexes that belong to EP_j , starting from the next node of V_2 , according to the direction of counter-clockwise, until the previous node of V_6 is traversed. So V_3, V_4, V_5, V_1 are inserted orderly. At last, we get the visibility region, which is a star-shaped polygon, namely, $(V_6, e, V_7, c, d, V_8, g, V_2, V_3, V_4, V_5, V_1)$, as shown in Figure 8(b).

Shortest path from SP to endpoint $CO_{i,k}$ in EP_j Obviously, this sub-problem can be reduced to the shortest path problem between two points in the plane in which there are a lot of line segment obstacles. Lee et al. [15] address shortest path among line segment obstacles but they limit to the obstacles being "parallel" line segments. Moreover, several papers [16,17] address shortest path

among rectilinear obstacles in which obstacles are “rectangles” (e.g., in VLSI design). In particular, there are a large number of literatures investigating shortest path among polygon obstacles in the past decades [18,19,20,21,22,23,24]. At first glance, the sub-problem also is different from theirs. Though it is so, one classical method based on graph theory can be used for tackling the sub-problem by minor modification [20]. On the whole, there are two main steps in order to tackle this sub-problem.

- **Step 1:** Constructing visibility graph.
- **Step 2:** To compute the shortest path based on standard shortest path algorithm such as Dijkstra algorithm [25].

Ray-sweeping discussed in previous paragraph also can be used for computing the visibility graph. For two endpoints that are from different line segments, if the two endpoints are visible each other, then we connect them, in this way, we will build the visibility graph in the end. Note that, besides the endpoints of all line segments that are locating in EP_j , the point SP also should be constructed in the visibility graph.

As an example, four line segments illustrate the obstacles, as shown in Figure 8(c), the polygon $(V_1, V_2, V_3, V_4, V_5)$ illustrates EP_j . Then, based on the method discussed above, we can get the visibility graph, in which $(a, b, c, d, e, f, g, h, V_1)$ are the vertexes, line segments (a, b) , (c, d) , (e, f) , (g, h) and all dotted lines are the edges, as shown in Figure 8(d).

The length of each edge in the visibility graph can be obtained by calculating the Euclidean distance. Therefore, resorting to the Dijkstra algorithm, we can compute the shortest path from SP to any endpoint of these line segment obstacles.

Remark 1. Since evaluating the shortest path for each pair of endpoints in S_j is based on the same visibility graph, we can construct the visibility graph at the first step in Figure 7, which will save much more time.

4.5 Data Representation and Geometry Operations

Data representation Up to now, we have presented the detailed algorithm for the FAR problem. In this subsection, we address another important issue, that is, how to represent the AR as well as related intermediate results such as AAR?

We observe that all geometries (e.g., AR, AAR) involved in our algorithm can be classified into three cases in terms of their boundaries: 1) the boundary is consisting of only straight line segments, or 2) the boundary is consisting of only circular arcs, or 3) the boundary is consisting of the blend of straight line segment(s) and circular arc(s). Therefore, we need an unified data structure to represent them. In particular, this data structure should be convenient for executing related geometry operations (e.g., computing “ $AAR \cup PV R_i.k$ ” as shown in line 10 of Figure 7).

As we know, the boundaries of traditional polygon can be represented by a series of vertexes. However, for polygon with circular arcs (called *circular-arc polygon*), this method is invalid since two vertexes in here cannot exactly determine a circular arc segment. Fortunately, we observe that two vertexes incorporated with an *appendix point* can exactly determine a circular arc segment. Taking the circular-arc polygon (grey region) in Figure 9 as an example, obviously, we cannot exactly represent it if we only use 7 vertexes, V_1, V_2, \dots, V_7 , the reason is that the circular arc $\widehat{V_1 V_7}$ is ambiguity, it may be a major arc or a minor arc. However, when we add an appendix point V_8 , then the circular arc $\widehat{V_1 V_8 V_7}$ is without ambiguity.

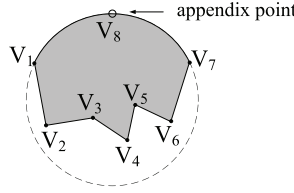


Fig. 9. Example of Circular-arc Polygon

In view of the above observation, we devise a data structure that can represent circular-arc polygon and traditional polygon in an unified manner, in this paper, we use a double linked list to represent them. The most key of point, comparing with the representation for traditional polygon, is that we add a 'tag' domain, which indicates whether a point is vertex or an appendix point. other domains are as similar as the traditional structure, e.g., 'data' domain is used for storing the coordination of vertex (or appendix point), i.e., (x_i, y_i) , 'pointer' domain is used for pointing to the previous/next vertex (or appendix point). For clearness, in the rest of this paper, an appendix point is denoted by $\overline{V_i}$, and a traditional vertex is denoted by V_i . For example, the circular-arc polygon (grey region) in Figure 9 can be denoted by $\{V_1, V_2, V_3, V_4, V_5, V_6, V_7, \overline{V_8}\}$.

Geometry operations In the sequel, we, based on the above data representation, address the geometry operations on circular-arc polygons. In particular, we mainly discuss computing the union between two circular-arc polygons, since it is a typical operation in the process of computing AR. On the whole, it involves the following two steps.

- **Step 1:** Computing all the intersections between two circular-arc polygons.
- **Step 2:** Constructing the resultant polygon based on these intersections and corresponding rules.

A simple method for calculating the intersections is to compare all the edge pairs of both polygons. However, this method bears a heavily time cost especially when the number of edges are much more. One elegant method for reporting the intersections among a set of segments is the *plane sweep algorithm* [26,27].

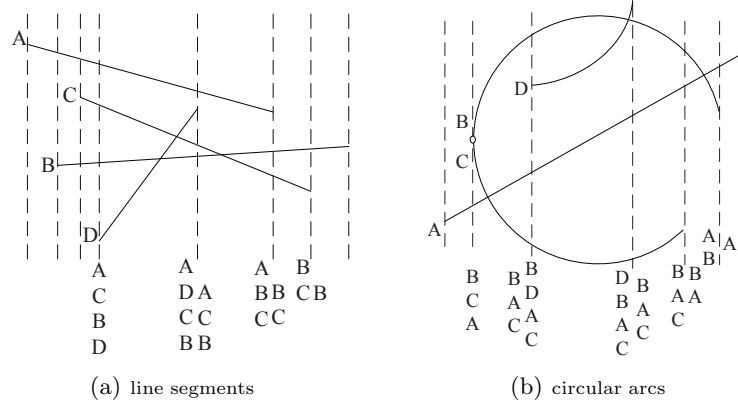


Fig. 10. Example of Plane Sweep

We, in here, present a modified version. The basic idea is as follows. Sorting the endpoints of all segments based on their x-coordinators at first. Next, the plane is swept (from left to right) with a vertical line. At every moment the line segments that intersect with the sweep-line are stored, ordered from bottom to top, in a data structure (e.g., a sequence linked list), *DS* for short. In particular, when the sweep line touches the left endpoint of a line segment, the line segment is put into *DS*. On the contrary, it is popped out from *DS* when the sweep line touches the right endpoint of this line segment. Therefore, the line segments stored in *DS* are changing dynamically. Note that, if the order of line segments in *DS* is changed when the sweep line moves from left to right, it must produce the intersection(s).⁴ So the intersections among line segments can be detected by observing whether the order of line segments (in *DS*) is changed, this is the main difference. (Note that, original algorithm always test if a new inserted line segment intersects with the above/below line segment. Analogously, when a line segment is popped out from *DS*, original algorithm also do this kind of test, the time for both of the tests can be save using the modified version.)

For example, on the 4th sweep line, line segments “A, C, B, D” are sorted (in *DS*) based on their y-coordinators, as shown in Figure 10(a). Next, on the 5th sweep line, the order of these four line segments takes place a change. Specifically, line segment D is promoted in two levels, so “D” must intersect with “B” and “C” in the interval between the 4th and 5th sweep line. By the way, “D” is popped out from *DS* after the 5th sweep line, then, the sequence is “A, C, B” now. On the 6th sweep line, the sequence is changed to “A, B, C”, we, similar to previous reason, can know that “B” must intersects with “C” in the interval between the 5th and 6th sweep line.

In here, we resort the principle of plane sweep method for finding the intersections between two circular-arc polygons. It is worth noting, since a circular arc possible intersects with the vertical line (or sweep line) at two points, it will make the plane sweep algorithm invalid. For tackling this problem, we, at first,

⁴ The complete proof can be found in literature [26].

decompose non-x-monotone circular arc (if exist) into two x-monotone circular arcs.⁵ Specifically, we use a horizontal line passing through the center of corresponding circle to decompose a non-x-monotone circular arc into two x-monotone arcs. For convenience, called them as *upper arc* and *below arc*, respectively.

Taking the big circular arc in Figure 10(b) as an example, which is a non-x-monotone arc, we decompose it into two arcs “*B*” (upper arc) and “*C*” (below arc). On the 2nd sweep line, the sequence stored in *DS* is “*B, C, A*”. For the 3rd sweep line, before putting “*D*” into *DS*, the sequence has changed to “*B, A, C*”, so we know “*A*” must intersects with “*C*” in the interval between the 2nd and 3rd sweep line. As the sweep line moves from left to right, similarly, we can know “*D*” intersects with “*B*”, and “*A*” intersects with “*B*”.

Once the intersections between two circular-arc polygons are obtained based on the above method, we then construct the resultant polygon. For traditional polygons, one classical method constructing resultant polygon is based on the so called *entry-exit* rules [28,29]. Their basic idea is as follows. Inserting the intersections into the two polygons, and marking these intersections with *entry* or *exit* property, next, traversing from a starting vertex along the edges, in which it shifts to traverse another polygon once it meets the *entry* or *exit* point, and vice versa. In the end a circuit is produced, this is just the boundary of resultant polygon.

In here, we extend this idea to our problem, but we have to do some additional efforts since the circular arcs present. The first effort is to sort intersections on a circular arc according to the direction of anti-clockwise, this is ready for inserting new *appendix point* and for traversing. The second effort is to insert new *appendix point* into the circular arc if there is(are) intersection(s) on it, this is ready for eliminating the ambiguity.

Lemma 7. *Given there are a number K of intersections on a circular arc, then it need insert at least K and at most $K + 1$ new appendix points for eliminating the ambiguity.*

Proof. Since K intersections can subdivide a complete circular arc into $K + 1$ small circular arcs, and for each small circular arc, one *appendix point* is needed and is enough to eliminate the ambiguity. So for $K + 1$ small circular arcs, $K + 1$ *appendix points* are needed and it is enough to eliminate the ambiguity. Further, since there is an *appendix point* beforehand. Therefore, when there is no intersection coinciding with this *appendix point*, only K new *appendix points* are needed. Otherwise, $K + 1$ new *appendix points* are needed. \square

For example, there are two circular-arc polygons, as shown in Figure 11, $CAP_1 = \{V_1, V_2, V_3, \overline{V_4}, V_5, V_6, \overline{V_7}, V_8, V_9, V_{10}\}$ and $CAP_2 = \{V_{11}, V_{12}, \overline{V_{13}}, V_{14}, V_{15}, V_{16}, V_{17}, \overline{V_{18}}, V_{19}, V_{20}\}$, in which we assume we have obtained the intersections between the two circular-arc polygons based on *sweep line* method. The black filled circle, black hollow circle, grey filled circle and grey filled circle with black

⁵ a x-monotone circular arc is such a circular arc that is at most one intersection with any vertical line.

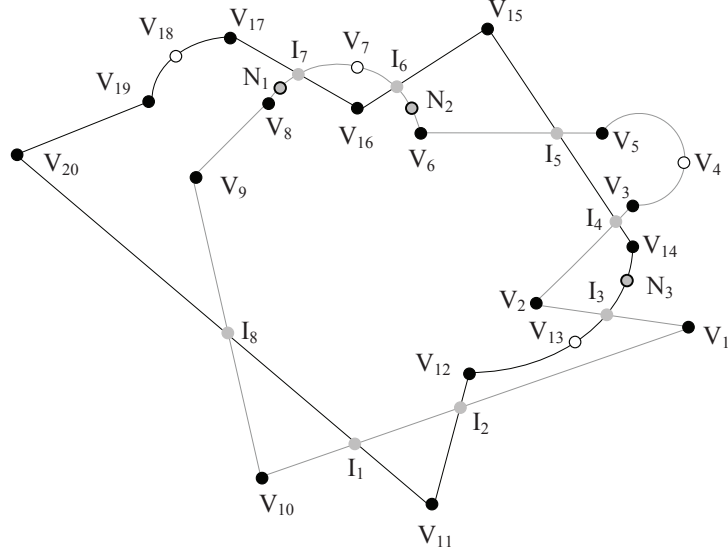


Fig. 11. Example of Constructing Resultant Polygon

edge denote vertexes, *appendix points*, intersections and new *appendix points*, respectively. For CAP_1 , on the arc $\widehat{V_6V_7V_8}$, there are two intersections I_6 and I_7 , we sort them according to the direction of anti-clockwise. In particular, we view this circular arc as three small circular arcs which are separated by the two intersections. So we insert two new *appendix points* N_1 and N_2 for eliminating ambiguity. Similarly, for CAP_2 , we view $\widehat{V_{12}V_{13}V_{14}}$ as two small circular arcs which are separated by the intersection I_3 , and we also insert a new *appendix point* N_3 .

After intersections and new *appendix points* are orderly inserted into the two initial circular-arc polygons separately, we get two new linked lists, then, we assign the intersections with *Entry* or *Exit* property alternately. At last, we traverse the two new linked lists and obtain the resultant polygon. For instance, in Figure 11, the new linked list (corresponding to CAP_1) is $\{V_1, I_3, V_2, I_4, V_3, \overline{V_4}, V_5, I_5, V_6, \overline{N_2}, I_6, \overline{V_7}, I_7, \overline{N_1}, V_8, V_9, I_8, V_{10}, I_1, I_2\}$, another new linked list (corresponding to CAP_2) is $\{V_{11}, I_2, V_{12}, \overline{V_{13}}, I_3, \overline{N_3}, V_{14}, I_4, I_5, V_{15}, I_6, V_{16}, I_7, V_{17}, \overline{V_{18}}, V_{19}, V_{20}, I_8, I_1\}$. We assign " I_1, I_2, \dots, I_8 " with "*entry, exit, \dots, exit*", respectively. Then, we traverse the first new linked list, starting from V_1 , along the direction of anti-clockwise. Once we meet a intersection with "*entry*" property, we shift to traverse the second new linked list. Similarly, once we meet a intersection with "*exit*" property (in the second new linked list), we shift to traverse the first new linked list, and so on. In the end, we get the resultant polygon, $\{V_1, I_3, \overline{N_3}, V_{14}, I_4, V_3, \overline{V_4}, V_5, I_5, V_{15}, I_6, \overline{V_7}, I_7, V_{17}, \overline{V_{18}}, V_{19}, V_{20}, I_8, V_{10}, I_1, V_{11}, I_2\}$, which is just the union of CAP_1 and CAP_2 .

In the process of computing *achievable region*, there are some other geometry operations, which possibly don't aim at two circular-arc polygons, or possibly is not computing the union of two geometries. In addition, some degenerations possible happen. For these issues, the complete description is beyond the scope of this paper, these can be either found in literatures [28,29], or easily deduced based on the above discussion. We, for saving space, don't further talk the details.

5 Correctness and Complexity

5.1 Proof of correctness

For proving the correctness of our proposed method, we only need to prove the following two propositions.

Proposition 1. *Any possible location (or point) at which one can reach is locating in AR.*

Proof. By contradiction. Given a point is achievable, we assume it is not locating in AR. Obviously, this point should be either outside the CAR or inside the CAR. If it is the former, the point must be unachievable since the *MPL* is the radius of CAR, it is contrary to the given condition. If it is the latter, this point should be inside one of sectors, S_j . Recall the algorithm `Framework_FAR` (cf. Figure 2), the AR is the union of all AARs, i.e., $AR = \bigcup_{j=1}^{\|SLs\|} AAR_j$, where AAR_j is the AAR in S_j . Further, we know $AAR_j \subseteq S_j$. So this point only can locate in the region " $S_j - AAR_j$ ".

Since we classify S_j into four cases (cf. Section 4.4). For case 1, the region " $S_j - AAR_j$ " is equal to \emptyset . Obviously, this point cannot locate in this kind of sectors. We assume this point lies in so called case 2 sector, the region " $S_j - AAR_j$ " don't equal to \emptyset , but any location inside the region " $S_j - AAR_j$ " is obviously unachievable because of the limitation of *MPL* and the impact of obstacle (cf. Figure 3(b)), it is contrary to the given condition. Further, we assume this point lies in so called case 3 sector, we also can easily and similarly derive that this point is unachievable, it is contrary to the given condition.

At last, we assume this point lies in so called case 4 sector, the region " $S_j - AAR_j$ " also don't equal to \emptyset . Recall our algorithm `computing_AAR` (cf. Figure 7), the AAR in S_j , i.e., AAR_j , is the union of all $PVR_{i.k}$. Since $PVR_{i.k}$ is the pruned visibility region, that is, the region that the point visibility region $VR_{i.k}$ (in polygon EP_j) subtracts the circle centering at the endpoint $CO_{i.k}$ with radius RWL , this ensures that all locations at which one can directly reach from the endpoint $CO_{i.k}$ within distance RWL are included in AAR_j . In addition, since we compute the $PVR_{i.k}$ for each endpoint in S_j only if RWL larger than 0, where RWL is the value that *MPL* minuses the shortest path from SP to $CO_{i.k}$, these ensure that all locations (in S_j) at which one can reach are included in AAR_j . Since we assume this point locates in the region " $S_j - AAR_j$ ", but any location in this region is obviously unachievable, it is contrary to the given condition. Hence, the proposition holds. \square

Proposition 2. *No exist a location (or point) at which one cannot reach is locating in AR.*

Proof. By contradiction. Given there is a possible point at which one cannot reach, we assume it is locating in AR. Obviously, this point should be inside the CAR since $AR \subseteq CAR$. More clearly, this point should locate in certain AAR_j ($\subseteq S_i$). Since we classify S_j into five cases (cf. Section 4.4), then, we, first of all, assume this point locates in so called case 1 sector (cf. Figure 3(b)), obviously, any point in this region is achievable, it is contrary to the given condition. Next, we assume this point locates in so called case 2 sector, the triangle region is AAR_j , obviously, any point in the triangle is achievable, it is contrary to the given condition. Further, we assume this point locates in so called case 3 sector, we also can easily and similarly derive that any point in AAR_j is achievable, it is contrary to the given condition.

At last, we assume this point locates in so called case 4 sector. Since $PVR_{i.k}$ is the region that the point visibility region $VR_{i.k}$ (in polygon EP_j) subtracts the circle centering at the endpoint $CO_{i.k}$ with radius RWL , and since RWL is the value that MPL minuses the shortest path (from starting point SP to this endpoint), these ensure any point in region $PVR_{i.k}$ is achievable. In addition, we know AAR_j is the union of all $PVR_{i.k}$ (cf. Figure 7), so any point in AAR_j is achievable. Since we assumed this point locates in AAR_j , then, this point is achievable, it is contrary to the given condition. Hence, this proposition holds. \square

5.2 Computational complexity analysis

The algorithm framework consists of six steps (cf. Figure 2), we analyse the computational complexity on each step, then get the total computational complexity by accumulating. For convenience, in the rest of the paper, we use *complexity* and *computational complexity* interchangeably, and we denote the complexity for initializing (line 1), pruning unrelated objects (line 2), slicing and placing (line 3), computing the AAR in S_j (line 5), computing the union of all AARs (line 6), and returning result by $C_{initial}$, C_{prune} , C_{sp} , C_{aar} , C_{union} and C_{return} , respectively. So, the total complexity, C_{FAR} , can be derived as follows.

$$C_{FAR} = C_{initial} + C_{prune} + C_{sp} + k * C_{aar} + C_{union} + C_{return} \quad (5.1)$$

where k is the number of sectors, it is equal to $\|SLs\|$. Obviously, both $C_{initial}$ and C_{return} are $O(1)$ time. In addition, in the worst case, there are a number N of COs in CAR, so we have

Corollary 3. *Given all the N obstacles are COs, namely, all obstacles lie in CAR, then there are at most $2*N$ slicing lines.*

Proof. Based on the condition $\|COs\| = N$ and Lemma 4, the proof can be derived. \square

Therefore, the Equation 5.1 can be rewrote as follows.

$$C_{FAR} = C_{prune} + C_{sp} + \max_{1 \leq k \leq 2N} \{k * C_{aar}\} + C_{union} \quad (5.2)$$

Complexity for pruning unrelated obstacles (C_{prune}) Recall algorithm for pruning unrelated obstacles (cf. Figure 4), the subprocedure `Handle_obstacles()` takes constant time, denoted by $O(c_1)$. So, at the worst case, that is, when *switch* always is equal to 0 (line 4), the **for** circulation (line 3-11) needs $O(k_1 * c_1)$ time, where $k_1 = \|\text{ICOs}\|$. In addition, classical R-tree for finding ICOs (line 1) takes $O(N)$ time at the worst case, and sort the ICOs (line 2) using classical Heapsort algorithm takes $O(k_1 * \log k_1)$ time at the worst case, and returning COs (line 13) takes $O(1)$ time. Thus, we have

$$C_{prune} = O(N + k_1 * \log k_1 + k_1 * c_1) \quad (5.3)$$

In particular, $\|\text{ICOs}\| = N$ in extreme case, so Equation 5.3 can be rewrote as follows.

$$C_{prune} = \max_{0 \leq k_1 \leq N} \{O(N + k_1 * (c_1 + \log k_1))\} \quad (5.4)$$

Complexity for slicing and placing (C_{sp}) Recall algorithm for slicing and placing (cf. Figure 6), to determine if an endpoint can produce a slicing line (line 5) takes $O(k_2)$ time at the worst case, where $k_2 = \|\text{COs}\|$. In addition, at the worst case, “ $CO.k \notin RLT$ ” always holds (line 4), namely, *RLT* always is equal to \emptyset , so we have to determine (for each endpoint) if it can produce a slicing line. Therefore, to find out all slicing lines (line 2-10) takes $O(2 * k_2 * k_2)$ time, i.e., $O(k_2^2)$ time. Dividing the CAR into multiple sectors (line 11) only need sort the slicing lines w.r.t. polar plane coordinate, which takes $O(k * \log k)$ time, where $k = \|\text{SLs}\|$. To compute the enlarged polygon of S_j takes constant time, denoted by $O(c_2)$, so “line 12-14” takes $O(k * c_2)$ time. Moreover, since EP_j at most have 7 edges as shown in Figure 5, to determine if CO lies in EP_j (line 17) takes constant time, denoted by $O(c_3)$. Therefore, placing COs in S_j (line 15-17) takes $O(k_2 * k * c_3)$ time. Last, returning $\sum_{j=1}^{\|\text{SLs}\|} S_j.CO_s$ takes $O(1)$ time. Then, we have

$$C_{sp} = O(k_2^2 + k * \log k + k * c_2 + k_2 * k * c_3) \quad (5.5)$$

In extreme case, $\|\text{COs}\| = \|\text{ICOs}\|$ and $\|\text{ICOs}\| = N$, at the same time, based on corollary 3, the Equation 5.5 can be rewrote as follows.

$$C_{sp} = \max_{0 \leq k_2 \leq N, 0 \leq k \leq 2N} \{O(k_2^2 + k * (\log k + c_2) + k_2 * k * c_3)\} \quad (5.6)$$

Complexity for computing the AAR (C_{aar}) Recall algorithm for computing AAR (cf. Figure 7), we construct visibility graph at the first step (as Remark 1 suggests) for improving efficiency, using ray-sweeping method to construct visibility graph takes $O((2 * k_3 + 1)^2 * \log(2 * k_3 + 1))$ time⁶, i.e., $O(k_3^2 * \log k_3)$ time, where $k_3 = \|S_j.CO_s\|$.

In addition, to compute the shortest path (line 4) using Dijkstra algorithm takes $O((2 * k_3 + 1)^2)$ time⁷, i.e., $O(k_3^2)$ time. For obtaining the visibility region

⁶ This can be derived based on literature [20], “ $(2 * k_3 + 1)$ ” is corresponding to the “ n ” in their paper, where n is the number of obstacle corners.

⁷ More details about computing the shortest path please refer to the book [30].

(line 6), we first find out so called case 1 and 3 rays, it takes $O((2*(k_3-1))^2)$ time. At the worst cases, all rays are so called case 1 and case 3 ray, sorting them takes $O(2*(k_3-1)*\log(2*(k_3-1)))$ time, next, constructing visibility region based on crossing points and endpoints takes $O(2*(k_3-1))$ time. Therefore, to compute the visibility region takes $O((2*(k_3-1))^2 + 2*(k_3-1)*\log(2*(k_3-1)) + 2*(k_3-1))$ time, i.e., $O(k_3^2 + k_3 * \log k_3 + k_3)$ time.

For computing “ $VR_{i.k} \cap tempC$ ” (line 9), we need compute the intersection(s) (between each edge of $VR_{i.k}$ and the circle $tempC$), and insert the intersection(s) into corresponding edge. Specifically, once we obtain intersection(s) between an edge and $tempC$, we insert the intersection(s) into this edge, then to deal with next edge, in this way, all the intersections can be orderly inserted into $VR_{i.k}$ after we dealt with all the edges of $VR_{i.k}$. At the worst case, the $VR_{i.k}$ has a number $2*(k_3-1) + \epsilon$ of edges, and each one at most intersects with the $tempC$ at two points, where ϵ is a small integer denoting the edges coming from EP_j . So, to compute the intersection(s) and insert them into $VR_{i.k}$ takes $O(k_3)$ time. Before we construct the result of “ $VR_{i.k} \cap tempC$ ”, we also have to sort all the intersections on the circle $tempC$ w.r.t. polar plane coordinate, it takes $O(k_3 * \log k_3)$ time, in addition, we insert the *appendix point* between each pair of intersections on the circle, it at most takes $O(k_3)$ time. Next, to construct the resultant polygon based on “*entry-exit*” rule, it needs traversing all endpoints (including so called *entry-exit* points), it at most takes $O(k_3)$ time. Therefore, to compute “ $VR_{i.k} \cap tempC$ ” takes $O(k_3 + k_3 * \log k_3 + k_3 + k_3)$ time, i.e., $O(k_3 + k_3 * \log k_3)$ time.

At the worst case, “ $STP < MPL$ ” always holds (line 5). Therefore, “line 2-10” takes $O(2 * k_3 * (k_3^2 + (k_3^2 + k_3 * \log k_3 + k_3) + (k_3 + k_3 * \log k_3)))$ time, i.e., $O(k_3^3 + k_3^2 * \log k_3)$ time.

Next, we analyse the complexity for computing all the union of pruned visibility region (line 11), which can be reduced to computing the union of two circular-arc polygons as discussed in Subsection 4.5.

Theorem 1. *Given two circular-arc polygons with m and n edges, respectively, and assume there is no non-x-monotone arc in the two polygons, then, to compute the intersections using the modified plane sweep method takes $O((m+n)*\log(m+n) + i)$ time, where i is the number of intersections.*

Proof. The proof is analogous to the argument in Theorem 3 of literature [27], we omit the details due to space limit. \square

Since a circular-arc polygon with m edges at most has a number m of non-x-monotone arcs, and to decompose a non-x-monotone arc takes constant time, then, based on Theorem 1, we have an immediate corollary below.

Corollary 4. *Given two circular-arc polygons with m and n edges, respectively, then, to compute the intersections using the modified plane sweep method takes $O((m+n) + ((m+n)*\log(m+n) + i))$ time, where i is the number of intersections.*

\square

To compute the union of all pruned visibility regions (PVRs), we use divide and conquer. At the worst case, “ $STP < MPL$ ” always holds (line 5), so, it runs $\log(2 * k_3 + 1)$ turns.

For each turn, since the number of edges in each PVR at most is equal to $4 * (k_3 - 1)$, the number of all intersections (among all edges from two PVRs) are $(4 * (k_3 - 1))^2$ at most⁸. Then, based on Corollary 4, we know that computing the intersections in each turn takes $O((8 * (k_3 - 1) + 8 * (k_3 - 1) * \log(8 * (k_3 - 1)) + (4 * (k_3 - 1))^2) * (2 * k_3 + 1) / 2)$ time, i.e., $O(k_3^3 + k_3^2 * \log k_3 + k_3^2)$ time. In addition, to insert the number $(4 * (k_3 - 1))^2$ of intersections into the two PVRs takes $O(k_3^3)$ time. At the worst case, all the intersections on an arc, then sorting these intersections takes $O(k_3^2 * \log k_3^2)$ time. Moreover, based on Lemma 7, to insert *new appendix points* takes $O(k_3^2)$ time at most. Further, since there are at most $2 * 4 * (k_3 - 1) + (4 * (k_3 - 1))^2$ endpoints (including the intersections and vertexes), to construct the resultant polygon based on “entry-exit” rule, it takes $O(k_3^2)$ time.

Therefore, to compute the union of all PVRs takes $O(\log(2 * k_3 + 1) * ((k_3^3 + k_3^2 * \log k_3 + k_3^2) + k_3^3 + k_3^2 * \log k_3^2 + k_3^2 + k_3^2))$ time, i.e., $O(\log k_3 * (k_3^3 + k_3^2 * (\log k_3 + \log k_3^2)))$ time. At last, returning the AAR (line 12) takes $O(1)$ time. Thus, we have

$$C_{aar} = O(k_3^2 * \log k_3 + (k_3^3 + k_3^2 + k_3^2 * \log k_3) + \log k_3 * (k_3^3 + k_3^2 * (\log k_3 + \log k_3^2))) \quad (5.7)$$

Similarly, at the extreme case, $\|S_j.COs\| = \|COs\|$ and $\|COs\| = N$, so Equation 5.7 can be rewrote as follows.

$$C_{aar} = \max_{0 \leq k_3 \leq N} \{O(k_3^2 * \log k_3 + (k_3^3 + k_3^2 * \log k_3) + \log k_3 * (k_3^3 + k_3^2 * (\log k_3 + \log k_3^2)))\} \quad (5.8)$$

Complexity for computing the union of all AARs (C_{union}) Since any two sectors at least have a common point, i.e., SP , and any two adjacent sectors have a common slicing line (SL). Based on this observation, we have

Theorem 2. *Given any two adjacent sector S_j and S_j^* , and given we have obtained the AARs in S_j and S_j^* , which are denoted by AAR_j and AAR_j^* , respectively. Further, given AAR_j and AAR_j^* consist of m and n vertexes (do not include the appendix points), respectively. To compute the union between AAR_j and AAR_j^* takes $O(m + n)$ time.*

Proof. To compute the union between AAR_j and AAR_j^* is different from that discussed in Subsection 4.5. Based on Corollary 2, we need find out the common edge between AAR_j and AAR_j^* , this common edge in fact is a SL. Since SP belongs to any SL, and we use double linked list to store the vertexes and appendix points, so we need to find out the vertex “ SP ” from the two double linked lists, it takes $O(m)$ and $O(n)$ time at the worst case. Then, to find out the common SL,

⁸ Note that, the intersections do not include the vertexes from two PVRs.

only 4 times comparisons are needed at the worst case since each AAR has two SLs, it takes $4 * O(1)$ time. At last, we combine the two linked lists in $O(1)$ time since we only need adjust the pointer of double linked list. To sum up, to compute the union between AAR_j and AAR_j^* takes “ $O(m) + O(n) + 4 * O(1) + O(1)$ ” time, i.e., $O(m + n)$ time. \square

To compute the union of all AARs, we first sort the AARs w.r.t. polar plane coordinate, it takes $O(k * \log k)$ time, where $k = \|\text{SLs}\|$. Then, we merge all the AARs using divide and conquer, it runs $\log k$ turns. For each turn, at the worst case, the number of vertexes for each AAR is equal to $2 * \|S_j.COs\| + 3$, then, based on Theorem 2, we know that merging in each turn takes $O((2 * k_3 + 3) + (2 * k_3 + 3)) * (k/2)$ time, i.e., $O(k_3 * k)$ time, where $k = \|\text{SLs}\|$, and $k_3 = \|S_j.COs\|$. Thus, we have

$$C_{union} = O(k * \log k + k_3 * k * \log k) \quad (5.9)$$

Further, based on Corollary 3, and $\|S_j.COs\| = \|\text{COs}\|$ and $\|\text{COs}\| = N$ at the extreme case, so Equation 5.9 can be rewrote as follows.

$$C_{union} = \max_{0 \leq k_3 \leq N, 0 \leq k \leq 2N} \{O(k_3 * k * \log k)\} \quad (5.10)$$

The total complexity (C_{FAR}) For Equation 5.2, we substitute C_{prune} , C_{sp} , C_{aar} , C_{union} with Equation 5.4, 5.6, 5.8 and 5.10, then, we have

$$\begin{aligned} C_{FAR} = & \max_{0 \leq k_1 \leq N} \{O(N + k_1 * (c_1 + \log k_1))\} \\ & + \max_{0 \leq k_2 \leq N, 0 \leq k \leq 2N} \{O(k_2^2 + k * (\log k + c_2) \\ & + k_2 * k * c_3)\} + \max_{0 \leq k_3 \leq N} \{O(k_3^2 * \log k_3 + (k_3^3 \\ & + k_3^2 * \log k_3) + \log k_3 * (k_3^2 * (\log k_3 + \log k_3^2) \\ & + k_3^3))\} + \max_{0 \leq k_3 \leq N, 0 \leq k \leq 2N} \{O(k_3 * k * \log k)\} \end{aligned} \quad (5.11)$$

By eliminating constant factor c_1 , c_2 and c_3 , the Equation 5.11 can be rewrote as follows.

$$\begin{aligned} C_{FAR} = & \max_{0 \leq k \leq 2N, 0 \leq k_1 \leq N, 0 \leq k_2 \leq N, 0 \leq k_3 \leq N} \{O(k_3^3 * \log k_3 \\ & + k_3^2 * \log k_3 * (\log k_3 + \log k_3^2) + k * \log k \\ & + k_2 * k + k * k_3 * \log k + k_1 * \log k_1 + N)\} \end{aligned} \quad (5.12)$$

where $k = \|\text{SLs}\|$, $k_1 = \|\text{ICOs}\|$, $k_2 = \|\text{COs}\|$, and $k_3 = \|S_j.COs\|$. It is worth noting that $k = 2N$ and $k_3 = N$ cannot be satisfied simultaneously. At extreme case, $k_1 = N$, $k_2 = N$ and $k_3 = N$ can be satisfied simultaneously, and we observe that there is no any slicing line (i.e., $k = 0$) when $k_3 = N$, at this time, Equation 5.12 has a maximum value, we substitute k, k_1, k_2, k_3 with $0, N, N, N$, respectively. So, we have

$$\begin{aligned} C_{FAR} = & O(N^3 * \log N + N^2 * \log N * (\log N + \log N^2) \\ & + N^2 + N * \log N + N) \end{aligned} \quad (5.13)$$

Thus, by O -notation, the total complexity is $O(N^3 \log N)$.

6 Conclusion

This paper proposes and formulates the FAR problem, we settle this problem under the assumption where the obstacles are line segments. A slice based method is presented, we demonstrate the correctness and the computation complexity of our proposed method by elaborate analysis. In future, we will investigate the FAR problem under the assumption where the obstacles are arbitrary polygons and delve into more efficient method.

References

1. ElGindy, H.A., Avis, D.: A linear algorithm for computing the visibility polygon from a point. *Journal of Algorithms (JAL)* **2**(2) (1981) 186–197
2. Welzl, E.: Constructing the visibility graph for n -line segments in $O(n^2)$ time. *Information Processing Letters (IPL)* **20**(4) (1985) 167–171
3. Lee, D.T., Lin, A.K.: Computational complexity of art gallery problems. *IEEE Transactions on Information Theory (TIT)* **32**(2) (1986) 276–282
4. pang Chin, W., Ntafos, S.C.: Optimum watchman routes. In: *ACM SIGACT/SIGGRAPH Symposium on Computational Geometry (SoCG)*. (1986) 24–33
5. Wang, B.: Coverage problems in sensor networks: A surveys. *ACM Computing Surveys (CSUR)* **43**(4) (2011)
6. Meguerdichian, S., Koushanfar, F., Potkonjak, M., Srivastava, M.B.: Coverage problems in wireless ad-hoc sensor networks. In: *IEEE International Conference on Computer Communications (INFOCOM)*. (2001) 1380–1387
7. Hwang, Y.K., Ahuja, N.: Gross motion planning - a survey. *ACM Computing Surveys (CSUR)* **24**(3) (1992) 219–291
8. Ghosh, S.K.: *Visibility algorithms in the plane*. Cambridge University Press, New York (2007)
9. O'Rourke, J.: *Art gallery theorems and algorithms*. Oxford University Press, Oxford (1987)
10. Ricci, A.: An algorithm for the removal of hidden lines in 3d scenes. *The Computer Journal (CJ)* **14**(4) (1971) 375–377
11. Eastman, J.F.: An efficient scan conversion and hidden surface removal algorithm. *Computers and Graphics (CG)* **1**(2-3) (1975) 215–220
12. Lingappan, L., Gangaram, V., Jha, N.K., Chakravarty, S.: Fast enhancement of validation test sets for improving the stuck-at fault coverage of rtl circuits. *IEEE Transactions on VLSI Systems* **17**(5) (2009) 697–708
13. Altshuler, D., Pollara, V.J., Cowles, C.R., Etten, W.J.V., Baldwin, J., Linton, L., Lander, E.S.: An snp map of the human genome generated by reduced representation shotgun sequencing. *Nature* **407** (September 2000) 513516
14. Andrews, J.H., Briand, L.C., Labiche, Y., Namin, A.S.: Using mutation analysis for assessing and comparing testing coverage criteria. *IEEE Transactions on Software Engineering (TSE)* **32**(8) (2006) 608–624
15. DT Lee, F.P.: Euclidean shortest paths in the presence of rectilinear barriers. *Networks* **14**(3) (1984) 393–410
16. Lee, D.T., Yang, C.D., Wong, C.K.: Rectilinear paths among rectilinear obstacles. *Discrete Applied Mathematics (DAM)* **70**(3) (1996) 185–215

17. Zheng, S.Q., Lim, J.S., Iyengar, S.S.: Finding obstacle-avoiding shortest paths using implicit connection graphs. *IEEE Transaction on CAD of Integrated Circuits and Systems (TCAD)* **15**(1) (1996) 103–110
18. Kapoor, S., Maheshwari, S.N., Mitchell, J.S.B.: An efficient algorithm for euclidean shortest paths among polygonal obstacles in the plane. *Discrete and Computational Geometry (DCG)* **18**(4) (1997) 377–383
19. Asano, T., Asano, T., Guibas, L.J., Hershberger, J., Imai, H.: Visibility-polygon search and euclidean shortest paths. In: *IEEE Symposium on Foundations of Computer Science (FOCS)*. (1985) 155–164
20. Sharir, M., Schorr, A.: On shortest paths in polyhedral spaces. In: *ACM Symposium on Theory of Computing (STOC)*. (1984) 144–153
21. Mitchell, J.S.B.: Shortest paths among obstacles in the plane. In: *ACM Symposium on Computational Geometry (SoCG)*. (1993) 308–317
22. Kapoor, S., Maheshwari, S.N.: Efficient algorithms for euclidean shortest path and visibility problems with polygonal obstacles. In: *ACM Symposium on Computational Geometry (SoCG)*. (1988) 172–182
23. Rohnert, H.: Shortest paths in the plane with convex polygonal obstacles. *Information Processing Letters (IPL)* **23**(2) (1986) 71–76
24. Storer, J.A., Reif, J.H.: Shortest paths in the plane with polygonal obstacles. *Journal of ACM (JACM)* **41**(5) (1994) 982–1012
25. Dijkstra, E.W.: A note on two problems in connexion with graphs. *Numerische Mathematik* **1** (1959) 269–271
26. Bentley, J.L., Ottmann, T.: Algorithms for reporting and counting geometric intersections. *IEEE Transaction on Computers (TC)* **28**(9) (1979) 643–647
27. Shamos, M.I., Hoey, D.: Geometric intersection problems. In: *IEEE Symposium on Foundations of Computer Science (FOCS)*. (1976) 208–215
28. Greiner, G., Hormann, K.: Efficient clipping of arbitrary polygons. *ACM Transactions on Graphics (TOG)* **17**(2) (1998) 71–83
29. Liu, Y.K., Wang, X.Q., Bao, S.Z., Gombosi, M., Zalik, B.: An algorithm for polygon clipping, and for determining polygon intersections and unions. *Computers and Geosciences (GANDC)* **33**(5) (2007) 589–598
30. Cormen, T.H., Leiserson, C.E., Rivest, R.L., Stein, C.: *Introduction To Algorithms*, Second Edition. The MIT Press, Cambridge (2001)